Variation in the connectivity of the isoenergetic surfaces of $Bi_{1-x}Sb_x$ alloys under uniaxial compression

N. B. Brandt, M. Yu. Lavrenyuk, N. Ya. Minina, and A. M. Savin

M. V. Lomonosov State University, Moscow

(Submitted 3 December 1988)
Zh. Eksp. Teor. Fiz. **94**, 235–248 (June 1988)

By subjecting single-crystal alloys of $Bi_{1-x}Sb_x$ ($0.2 \leqslant x \leqslant 0.3$) to uniaxial compression along the twofold and bisector axes up to a deformation of $\sim 0.3\%$, we have observed electronic topological transitions consisting of (1) pairwise coalescence of the two identical isoenergetic ellipsoidal surfaces at the L-point into a single dumbbell-shaped surface ($x < 0.25$), and (2) disruption of the "neck" of a normally dumbbell-shaped Fermi surface ($x > 0.25$). In the neighborhood of these transitions we observe anomalies in the thermoelectric power and resistivity; in a magnetic field, we observe the phenomenon of intraband magnetic breakdown. The data we have obtained point to the existence of a saddle point in the energy spectrum of $Bi_{1-x}Sb_x$ alloys with $x \geqslant 0.2$ and to a spectrum of inverted character in the range of antimony concentrations $x > 0.04$.

1. INTRODUCTION

The alloys $Bi_{1-x}Sb_x$ form substitutional solid solutions over the whole range of concentrations x; as x increases, the energy spectra of these alloys continuously transform from the spectrum of Bi to the spectrum of Sb. The semimetallic properties of $Bi_{1-x}Sb_x$ in the interval $0 \leqslant x \leqslant 0.65$ are connected with a slight overlap of the three band extrema at the L-points of the Brillouin zone, corresponding to three isoenergetic surfaces in the form of triaxial ellipsoids, with a hole-band extremum at the T-point. The magnitude of this overlap decreases with increasing x, and for $0.065 \leqslant x \leqslant 0.22$ the alloy $Bi_{1-x}Sb_x$ is a semiconductor with a direct gap E_{gL}. For concentrations $x \geqslant 0.22$, the L-extrema overlap with a new hole-band term, which according to the data of Ref. 1 corresponds to the term at the H-point in pure antimony. At $x = 0.04$ the electron and hole terms at the L-point cross in energy (i.e., $E_{gL} = 0$).

Up until recently the prevailing band-structure models for these systems[1,2] suggested that the spectra of Bi and the alloys $Bi_{1-x}Sb_x$ for $x < 0.04$ are inverted ($E_{gL} < 0$), while the spectrum of Sb is direct ($E_{gL} > 0$). There is no direct experimental evidence for these assertions,[1)] although several papers have reported positive values of E_{gL} obtained from band-structure calculations of Bi.[5,6]

Not long ago, Refs. 7, 8 reported data indicating that a saddle point is present in the energy spectrum of $Bi_{1-x}Sb_x$ for $x > 0.15$; such a point qualitatively changes the picture of the band structure, in particular the character of the band inversion at the L-point for $x = 0.04$. According to these data, the function $E(K)$ for $x > 0.15$ acquires a two-humped form (Fig. 1a), while in the semimetallic region $x > 0.22$ the isoenergetic surfaces at the L-point assume a dumbbell shape at the instant when the Fermi level passes through the saddle point in the spectrum. This happens for a certain critical concentration $x_{cr} \approx 0.25$.[7]

There is considerable interest in subjecting samples of $Bi_{1-x}Sb_x$ alloys with $x > 0.2$ to uniaxial strain in order to investigate the topology of their isoenergetic surfaces in detail at the L-point; strain makes it possible to observe the change in the shape of the isoenergetic surfaces at the L-point as the Fermi energy is monotonically varied, without changing the alloy composition.

To this end, we investigated the Shubnikov-deHaas (SdH) effect in the course of this work; we also measured the thermoelectric power and resistivities of $Bi_{1-x}Sb_x$ samples in the concentration interval $0.21 \leqslant x \leqslant 0.3$ for uniaxial compression along the twofold (C_2) and bisector (C_1) axes. For this type of strain, the previously equivalent band extrema diverge at a rate of 1.1 and 1.0 eV per unit strain for $\sigma \| C_2$ and $\sigma \| C_1$ respectively, where σ is the direction of compression.[9] The character of this motion of the L-terms with strain is shown in Figs. 1b; it leads to the unique possibility of passing the Fermi level in one (L_1) or two ($L_{2,3}$) equivalent extrema through the postulated saddle point in the course of a single experiment, and of observing the corresponding variation of the Fermi surface (FS). The formation (or disruption) of the dumbbell, which according to Ref. 7 we should expect to occur at a certain strain $\varepsilon = \varepsilon_{cr}$, constitutes an electronic topological transformation (ETT) of Lifshits type[10] and should be accompanied by anomalies in the thermolectric power and resistivity.[11–13] Therefore, investigations of these critical characteristics, together with study of the topology of the FS, give additional information about the presence or absence of a saddle point in the energy spectrum of a given

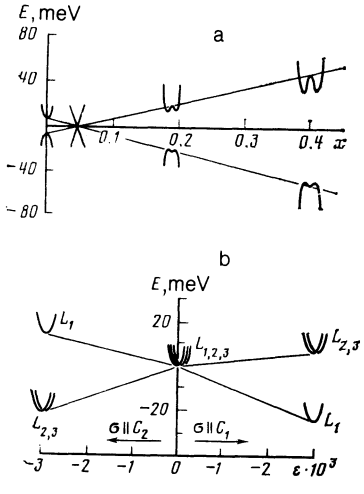

FIG. 1. (a) Variation of the energy spectrum at the L-point of $Bi_{1-x}Sb_x$ alloys with composition.[7] (b) Relative shift of the L-terms for $Bi_{1-x}Sb_x$ alloys ($0 \leqslant x \leqslant 0.1$) under uniaxial compression along C_1 and C_2.

 0038-5646/88/061220-09$04.00

alloy. Observation of anomalies in the thermoelectric power and resistivity as the "neck" of the dumbbell forms and is disrupted in the course of continuous elastic deformatiown of the sample is of interest in its own right, because in contrast to ETTs of the "FS sheet generation" type[14,15] this type of transition has been almost unstudied.[2)] Analysis of our results was carried out according to McClure's model of the energy spectra of Bi and $Bi_{1-x}Sb_x$ alloys.[17]

2. EXPERIMENTAL METHODS. SAMPLES

Single-crystal alloys of $Bi_{1-x}Sb_x$ with antimony concentrations in the range $0.2 \leqslant x \leqslant 0.3$ were grown by the zone recrystallization method at the Humboldt University in Berlin. The antimony concentration in the alloys was controlled by radiography to an accuracy of 0.3% by measuring the spacing d between (111) lattice planes, using data on the function $d(x)$ given in Ref. 18. The samples were cut off using the electric-spark method from a bulk boule and were oriented according to the tracks of secondary cleavage planes in the basal plane with the help of a binocular microscope to an accuracy of $\sim 1°$.

Control of the size and shape of the FS was implemented using the SdH effect, whose investigation was carried out by the standard method of low-frequency modulation of the magnetic field H at a frequency of 23 GHz under constant-current conditions in DC fields up to 56 kOe. The accuracy to which the FS cross-sectional area is determined depends on the complexity of the SdH oscillations and the field interval over which they are observed. For single-frequency SdH curves it amounts to 2–3%, while in the presence of beat frequencies it is 8–12%.

The methods of producing the uniaxial strain and measuring the thermoelectric power and resistivity under deformation are analogous to those described in Ref. 15. The temperature difference ($\Delta T \sim 0.2$K) was measured with a Cu–CuFe thermocouple, whose copper junctions served as potential contacts. The thermoelectric power signals from the sample and from the thermocouples were amplified with an F116/1 photomultiplier and recorded with a digital voltmeter. The measurement accuracy for the thermoelectric power signal amounted to $\sim 2.10^{-9}$ v/K.

3. EXPERIMENTAL RESULTS

According to Ref. 7, the Fermi level passes through the saddle point of the spectrum E_{cr} at a concentration $x_{cr} = 0.25$. For this reason, we studied two groups of $Bi_{1-x}Sb_x$ samples: group I with $0.21 \leqslant x \leqslant 0.23$, i.e., $x \leqslant x_{cr}$, and group II with $0.27 \leqslant x \leqslant 0.3$, i.e., $x > x_{cr}$. In group I, the Fermi level is located below the saddle point, while for group II it is above; this allows us to observe the "bridge formation (or disruption)" type of ETT both as the Fermi surface increases and as it decreases.

3.1. $Bi_{1-x}Sb_x$ alloys with concentrations in the range $0.21 \leqslant x \leqslant 0.23$

Investigation of these alloys is most conveniently carried out by compressing them along the bisector axis, since their compositions put them in the immediate vicinity of a semiconductor ($x < 0.22$–metal ($x > 0.22$) transition. If this transition is induced using uniaxial strain along C_1, then because of the divergence of the L-terms (Fig. 1b), the makeup of the electronic FS is determined by the L_1 extremum alone.

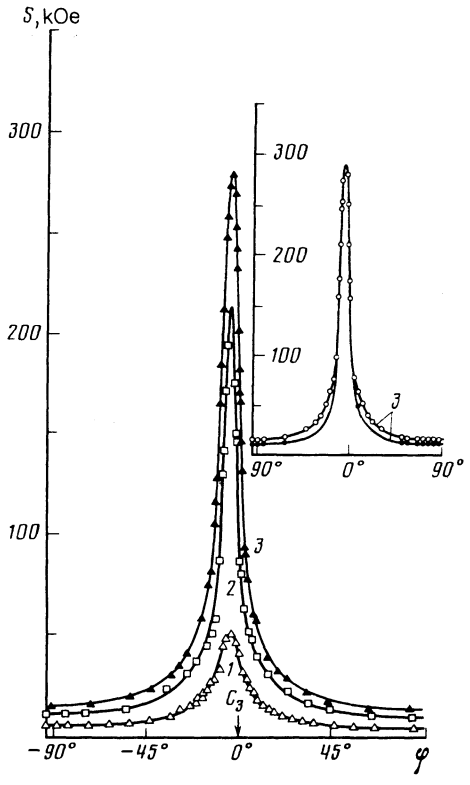

FIG. 2. Angular dependence of the extremal cross sections of the electron FS in the (C_1, C_3) plane for compression of a $Bi_{0.77}Sb_{0.23}$ sample along C_1: 1—$\varepsilon = -1 \cdot 10^{-3}$, 2—$\varepsilon = -2 \cdot 10^{-3}$, 3—$\varepsilon = -2.6 \cdot 10^{-3}$. The solid curves are calculations using the model of Ref. 17. The branches (and experimental points) which correspond to the formation of the neck of the dumbbell in cases 2 and 3 are presented only in the inset for case 3, i.e., when $\varepsilon = -2.6 \cdot 10^{-3}$.

This considerably simplifies the interpretation of the results: in place of a FS consisting of six pairwise-equivalent ellipsoids which, according to Ref. 7, arise because of the overlap with the hole-band H-term, the FS is made up of only two ellipsoids in the strained crystal. Furthermore, only one branch of SdH frequencies is connected with them.

Figure 2 shows the angular dependences of the extremal cross sections $S(\varphi)$ for samples of $Bi_{0.77}Sb_{0.33}$, where φ is the angle between **H** and $C3$; the $S(\varphi)$ were observed in the trigonal bisector plane at various strains. For all ten investigated samples in group I the variation in the FS with strain could be characterized by the following well-defined and generic regularities:

1. In the initial strain regime (i.e., immediately after electrons have overflowed the $L_{2,3}$ extrema into the L_1; for an initial carrier concentration $n_e \sim 10^{15}\text{cm}^{-3}$, this occurs at $\varepsilon \lesssim 0.2 \cdot 10^{-3}$ for the group-I alloys), the SdH oscillation curves are single-frequency for any direction of magnetic field. The angular dependences of this single frequency F are described by a single branch (curve 1 in Fig. 2).

2. All cross sections of the isoenergetic surface $S = (e\hbar/c)F$ rapidly increase with strain (Fig. 2).

3. For those orientations of the magnetic field corresponding to the regions of minimal cross-section ($\varphi \approx 90° \pm 30°$ in Fig. 2), a new, lower frequency appears in the oscillation curves as the strain increases. The angular dependence of this frequency is shown in the inset of Fig. 2. Its appearance indicates the formation of a second extremal

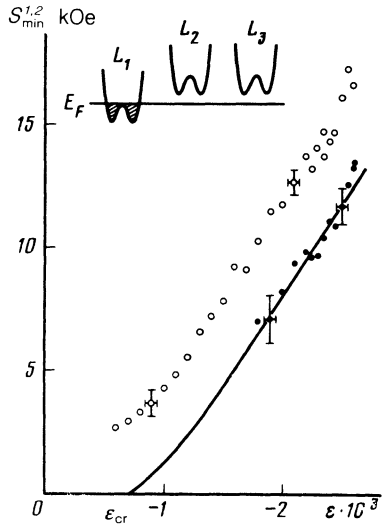

FIG. 3. Dependence of the minimum FS cross sections on strain in the alloy $Bi_{0.78}Sb_{0.22}$ for $\sigma \| C_2$: O—the body cross section $S^{(2)}_{min}$, ●—the neck cross section $S^{(1)}_{min}$. The solid curve comes from the model in Ref. 17 for the experimental dependence of $S^{(2)}_{min}(\varepsilon)$. In the inset we show a sketch of the shift in the L-terms near the Fermi level.

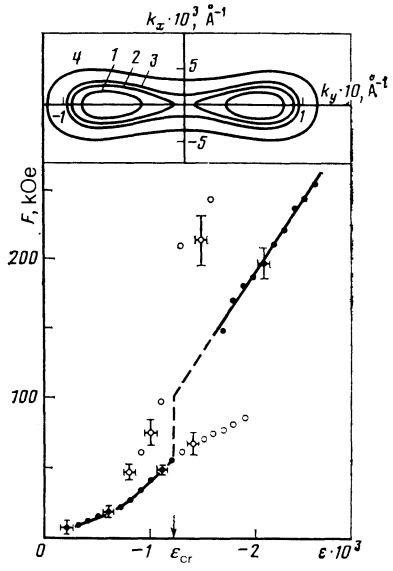

FIG. 5. Dependence of the SdH frequencies observed in the direction of maximum FS cross section on strain in the plane (C_1, C_3) for the alloy $Bi_{0.78}Sb_{0.22}$ ($\sigma \| C_1$): ●— frequencies from the maximum FS cross section, O—magnetic-breakdown frequencies. In the inset are shown cross section contours of the FS in the wave-vector plane (k_x, k_y), calculated using the model in Ref. 17 for E_F: 1—19 meV, 2—21.5 meV, 3—23 meV, 4—30 meV.

cross section for directions of magnetic field close to the direction of elongation of the isoenergetic surface. The lower frequency must be connected with $S^{(1)}_{min}$ ($K_y = 0$) for the central extremum of the dumbell surface, while the higher frequency is connected with $S^{(2)}_{min}$ for the non-central extremum ($K_y \neq 0$). These extrema arise when the two electronic sheets coalesce: $S^{(1)}_{min}$ is for the "neck" of the dumbbell and $S^{(2)}_{min}$ is for the "belly" (see the inset in Fig. 5). The dependences of $S^{(1)}_{min}$ amd $S^{(2)}_{min}$ on strain are shown in Fig. 3. It is clear that both the "belly" and the "neck" of the dumbbell grow at the same rate in the interval of strain under study, while the ratio $S^{(1)}_{min}/S^{(2)}_{min}$ decreases.

4. As the magnetic field is rotated in the (C_1, C_3) plane, the anisotropy in the cross-sections of each of the two isoenergetic surfaces up to their point of coalescence (the small-deformation portion of curve 1 in Fig. 2) has the value $A = S_{int}/S^{(1)}_{min} = 11$, where S_{int} is the maximum cross section for a quasiellipsoidal surface in this plane. This anisotropy is close to the corresponding value of A for pure Bi. At a certain strain $\varepsilon = \varepsilon_{cr}$, which depends on the antimony concentration and is determined by the value of E_{cr}, the anisotropy A discontinuously increases by a factor of 2, and then decreases for subsequent values of the deformation. In Fig. 4 we show the quantity A as a function of E_F at the L_1 extremum for a series of samples with $x = 0.21$, 0.22, 0.23. The sharp increase in the anisotropy with strain can also be seen if we compare curves 1 and 2 in Fig. 2.

5. The strain dependence of those oscillation frequencies which correspond to the maximum cross section S_{int} in the (C_1, C_3) plane has a complicated form (Fig. 5). At a deformation $\varepsilon \approx -0.8 \cdot 10^{-3}$, the single-frequency oscilla-

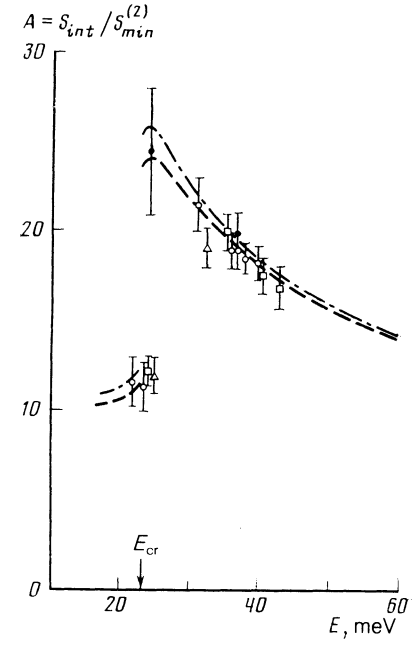

FIG. 4. Fermi energy dependence of the anisotropy in the cross sections of isoenergetic surfaces at L_1 in the (C_1, C_3) plane for the alloys: O—$Bi_{0.77}Sb_{0.23}$, □—$Bi_{0.78}Sb_{0.22}$, △—$Bi_{0.79}Sb_{0.21}$, ●—$Bi_{0.79}Sb_{0.21}$ (E_F changes under the compression $\sigma \| C_1$). The dashed and dot-dashed lines are calculated using the model of Ref. 17 for $Bi_{0.77}Sb_{0.23}$ and $Bi_{0.78}Sb_{0.22}$, respectively.

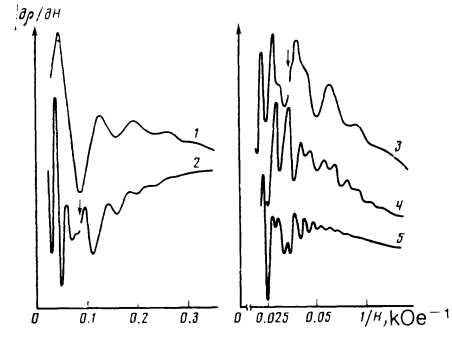

FIG. 6. Oscillations in the magnetoresistance corresponding to the data of Fig. 5: 1—$\varepsilon = -0.05\%$, 2—$\varepsilon = -0.08\%$, 3—$\varepsilon = -0.15\%$, 4—$\varepsilon = -0.19\%$, 5—$\varepsilon = -0.25\%$.

tions in the region of small loads (curve 1 in Fig. 6) and high magnetic fields change over to an oscillatory function consisting of two frequencies which differ in size by a factor of two (curve 2 in Fig. 6). In the strain interval $1.2\cdot10^{-3}\leqslant|\varepsilon|\leqslant1.6\cdot10^{-3}$ (Fig. 5), the doubled frequency disappears, and in its place there appear higher harmonics (curve 3 in Fig. 6). For a further increase in strain, there again appear two frequencies which differ by a factor of two (curve 5 in Fig. 6); in contrast to curve 2 in Fig. 6, the contribution of the lower frequency is apparent only for high magnetic fields. This variation in the overall picture of the oscillations with strain can be explained by intraband magnetic breakdown, which will be investigated below. As a consequence of this, a portion of the observed frequencies (denoted by the light points in Fig. 5) is related to magnetic breakdown, whereas only the function $F(\varepsilon)$, denoted in Fig. 5 by the solid line, is associated with the FS cross section S_{int}. The jump which this function undergoes at the point ε_{cr} is connected with the coalescence of the two quasiellipsoidal sheets at L into a single dumbbell, and with the formation of an electron orbit with twice the area as a result of this.

In our investigations of the thermoelectric power, we observed that as the strain increased the initially negative value of the signal decreased in absolute value. Against a background of monotonically-increasing values of the thermoelectric power with strain, we observed a marked negative-polarity peak in the neighborhood of $\varepsilon\approx-1.11\cdot10^{-3}$.

3.2. $Bi_{1-x}Sb_x$ alloys with concentrations in the range $0.27\leqslant x\leqslant0.3$

Our most complete results for the group-II samples are obtained for alloys with $x=0.27$. We investigated eight samples with this composition under compression along the C_1 and C_2 axes. According to the picture in Ref. 7, the FS of electrons for $Bi_{1-x}Sb_x$ with $x>0.25$ consists of three dumbbell-shaped surfaces at the L-points of the Brillouin zone. Uniaxial compression along the bisector axis must cause a decrease in the Fermi energy for two of the three previously equivalent L-extrema; in the same way, compression along the twofold axis decreases the Fermi energy for one of the extrema (see Fig. 1b). Therefore, we can expect that at a certain well-defined strain along one of these axes the Fermi level in the corresponding extrema decreases so much that it crosses the saddle point in the spectrum, i.e., $E_F=E_{\text{cr}}$. As a result, each of the dumbbell-shaped surfaces splits into two quasiellipsoids.

We studied the angular dependence of the extremal cross section of the FS for a sample compressed along C_1 as H was rotated in the (C_1, C_3) plane. This dependence is shown in Fig. 7 for an unstrained sample of $Bi_{0.73}Sb_{0.27}$: curve 1 corresponds to the two surfaces at $L_{2,3}$, which are decreasing as the strain along C_1 increases, while curve 2 is for the increasing part of the FS at l_1.

The distinctive feature of the oscillatory magnetoresistance functions in samples with concentrations $x>0.25$ compared to what is observed in pure bismuth is their increasing complexity, involving beating among the curves corresponding to the regions of minimum cross section. The difference manifests itself in the presence of a new low-frequency component which in group I samples appeared only under load (Fig. 3). In Fig. 7 we illustrate the angular dependence of this frequency (branch 2* of curve 2), while in

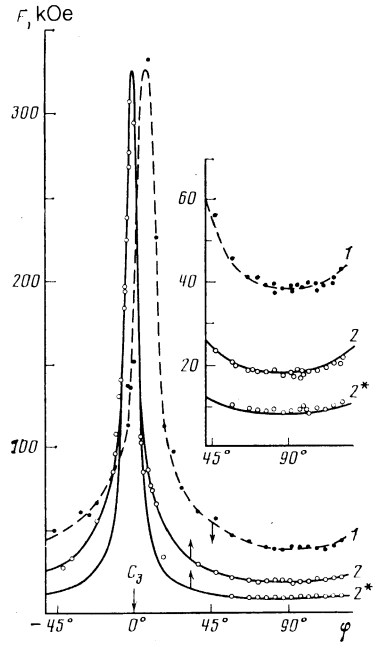

FIG. 7. Angular dependence of the extremal FS cross sections for the alloy $Bi_{0.73}Sb_{0.27}$ in the plane (C_1, C_3) for $\varepsilon=0$. The dashed curve is a plot of the experimental points, the solid curve (branches 2, 2*) is calculated using the model in Ref. 17. The arrows show the shift of the corresponding branches for a compression $\sigma\|C_1$.

Fig. 8 we show the characteristic SdH oscillations originating from the minimum cross sections. The presence of the new low-frequency component and the character of its angular dependence indicate that in type-II alloys the isoenergetic surfaces at L are dumbbell-shaped in the undeformed state $(E_F>E_{\text{cr}})$. The low frequency corresponds to the "neck" of the dumbbell-shaped surface at L_1: the experimental points lie on the theoretical function $S(\varphi)$, which was calculated using the model of Ref. 17 for this portion of the FS (Fig. 7, curves 2, 2*). In the region of minimal cross section there should be present a fourth frequency arising from the "necks" of the surfaces at $L_{2,3}$; however, it is close to the oscillation frequency for the "belly" at L_1 and thus was not resolved.

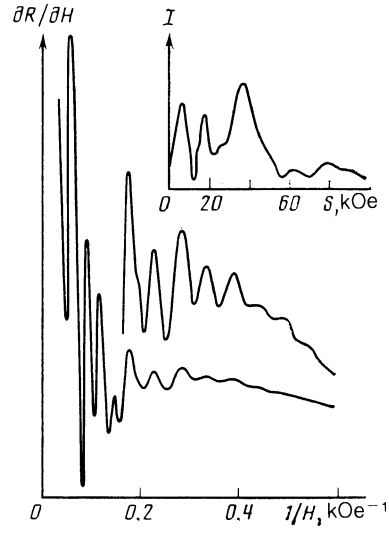

FIG. 8. SdH oscillations for $Bi_{0.73}Sb_{0.27}$ at $\varphi=100°$ (Fig. 7); the part of the curve for low fields is described with a higher sensitivity. In the inset we show the Fourier spectrum of the curve.

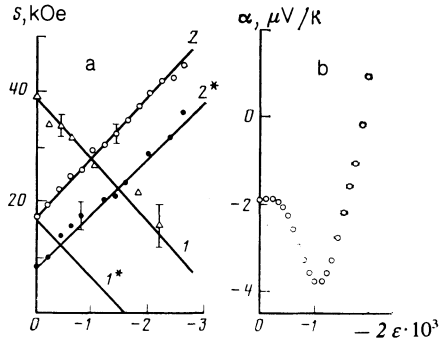

FIG. 9. (a) Dependence on strain of the minimum FS cross sections for $\sigma \| C_1$ in the alloy $Bi_{0.73}Sb_{0.27}$ ($\varphi = 90°$ in Fig. 7). (b)—Dependence on strain of the thermoelectric power signal in this sample.

The dependence of the FS cross-section on strain for $\varphi = 90°$ is shown in Fig. 9a. The "belly" and "neck" cross sections of the dumbbell at L_1 (curves 2 and 2*) increase with strain, while for those at $L_{2,3}$ the "belly" cross section decreases (curve 1). The disruption of the dumbbell at the $L_{2,3}$ extrema should be accompanied by a discontinuous decrease in its maximum cross section by a factor of two. However, for a given orientation of the sample, observation of this effect is hindered by that fact that curves 1 and 2 in Fig. 7 are shifted towards one another under strain. This complicates the resolution of the oscillatory dependences of the magnetoresistance from two neighboring and varying frequencies. The clearly marked negative-polarity peak which is observed in the dependence of the thermoelectric power signal on strain at $\varepsilon \approx -10^{-3}$ (Fig. 9b) indicates that such a disruption does take place. When the magnitude of the strain is further increased, the thermoelectric power signal passes through zero and becomes positive.

For compression along the C_2 axis we studied the angular dependence of the extremal cross sections of the Fermi surface as the magnetic field was rotated in the plane defined by the trigonal and twofold axes. In this orientation the oscillations from the increasing ($L_{2,3}$) and decreasing (L_1) parts of the Fermi surface are strongly separated in frequency over a rather wide range of angles, which makes it possible to observe the dependence of the decreasing maximal cross-section on strain without any particular difficulty. It should be pointed out that for a given orientation the minimum cross section of the decreasing FS is not observed, because the direction of the magnetic field is always practically perpendicular to the axis of its maximum elongation.[3)] This latter circumstance, however, makes this orientation particularly convenient for studying the behavior of the maximum cross-sections during the process of disruption of the electronic dumbbell.

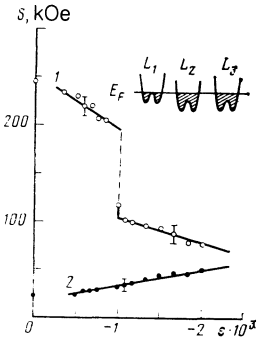

FIG. 10. Strain dependences of the FS cross sections for the alloy $Bi_{0.73}Sb_{0.27}$ in the direction $\mathbf{H} \perp C_1$; the angle between $\mathbf{H}$ and $C_3 = 30°$; $\sigma \| C_2$. In the inset we show the positions of the L-extrema at the instant the Fermi level passes through the saddle point at the L_1 extremum.

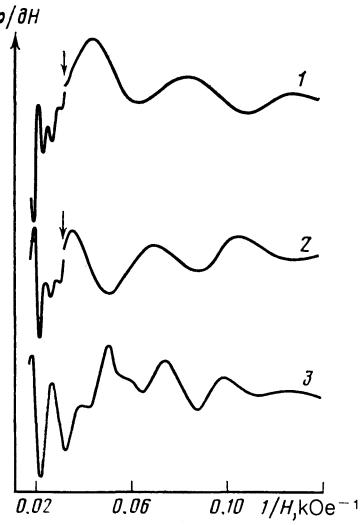

FIG. 11. SdH oscillations in the neighborhood of the jump in frequency (curve 1 in Fig. 10); 1—$\varepsilon = 0$, 2—$\varepsilon = -0.065\%$, 3—$\varepsilon = -0.13\%$.

The best separation of the increasing and decreasing frequencies of oscillation for rather large amplitudes of the latter took place in the vicinity of $\varphi = 30°$ (the angle is measured from the C_3 axis). The corresponding dependence of the extremal cross section on strain is shown in Fig. 10. For $\varepsilon \approx -10^{-3}$ we observed a discontinuous decrease in the oscillation frequency by a factor of two, connected with the maximal cross section of the decreasing part of the FS (curve 1). The increasing part of the FS varied monotonically in this case (curve 2).

The SdH oscillations in the region of the singularity in curve 1 of Fig. 10 are shown in Fig. 11. The oscillatory dependence of the magnetoresistance is a superposition of two components: the low frequency corresponds to the increasing part of the FS, while the high frequency is from the decreasing part (curve 1 in Fig. 10). For small variations in the strain, e.g., for $\Delta\varepsilon \approx 0.5 \cdot 10^{-4}$, the high frequency decreases by a factor of two in the vicinity of $\varepsilon \approx -10^{-3}$ while the low frequency remains almost unchanged.

On all samples with this orientation, we observed an irregularity in the behavior of $R(\varepsilon)$ in the vicinity of the strain $\varepsilon_{cr} \approx -10^{-3}$, taking the form of a washing-out of the step (Fig. 12a). As for the thermoelectric power signal in the neighborhood of ε_{cr}, we observed a negative-polarity peak, which was small but clearly marked and reversible with deformation (Fig. 12b). Just as for deformations along the C_1 axis, the signal passed through zero, changing its polarity to positive.

For $Bi_{1-x}Sb_x$ samples with $x \approx 0.3$, in which according to our SdH data the Fermi level was located 20 meV above the saddle point, no ETT of "broken-bridge" type was observed in the range of strains we studied, and no anomalies were observed in the quantities under discussion for these samples.

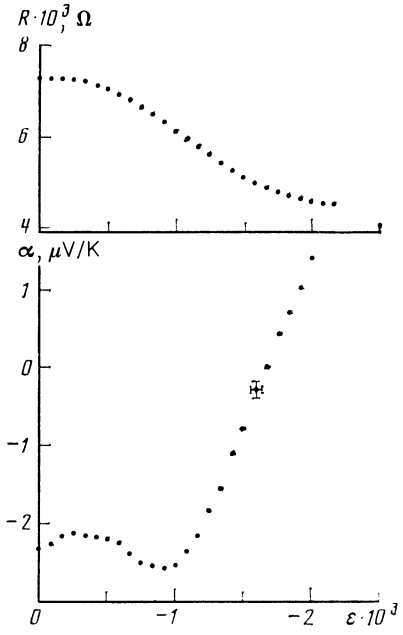

FIG. 12. Behavior of the thermoelectric power and resistivity in the neighborhood of the "broken bridge" type of ETT.

4. DISCUSSION OF RESULTS

4.1. Structure of the spectrum of $Bi_{1-x}Sb_x$ alloys with concentrations $0.2 \leqslant x \leqslant 0.3$

The totality of our experimental data agrees with the picture given in Ref. 7 of an energy spectrum of inverted ($E_{gL} < 0$) character in $Bi_{1-x}Sb_x$ alloys with $x \geqslant 0.04$ ($x = 0.04$ is the point where the bands cross each other); this results in the appearance of a saddle point at L in the spectrum of electrons and holes. The clearest experimental evidence for the existence of such a saddle point is the observed formation (in the group I samples) and disruptioon (in the group II samples) of a dumbbell-shaped isoenergetic surface which occurs under uniaxial strain, as observed in this work.

We call attention to the fact that the low-frequency component in the SdH oscillation spectrum, which is associated with the "neck" of the dumbbell-shaped surface (Figs. 2, 3, 7–9), cannot be connected with the hole part of the FS which arises from the semiconductor-metal transition for $x \geqslant 0.22$. In Refs. 1 and 19, in which the energy spectra of $Bi_{1-x}Sb_x$ alloys were studied in the concentration region $0.25 \leqslant x \leqslant 1$, it was shown that the hole isoenergetic surfaces for bismuth–antimony alloys in this concentration region[4)] are genetically related to the hole surfaces of antimony, which are determined by the terms at H. The cross sections of these surfaces, just as those of antimony, have a sharp angular dependence for magnetic field orientations close to the bisector direction, while the experimentally observed low frequency is almost independent of angle in this region. The low-frequency component also cannot be related to the hole surface at L, since the magnitude of the gap E_{gL} considerably exceeds the magnitude of the shift in the L terms with uniaxial compression.

4.2. Calculations based on the McClure model and experimental data

The following is a simplified form of the McClure dispersion law[17]:

$$(E+E_{gL}/2+\alpha_v k_y^2/2)\,(E-E_{gL}/2 -\alpha_c k_y^2/2) = Q_{11}^2 k_x^2 + Q_{22}^2 k_y^2 + Q_{33}^2 k_z^2, \quad (1)$$

where $\mathbf{k}$ is the wave vector measured from the L-point and E_{gL} is the direct gap at the L-point. The energy E is measured from the middle of the gap E_{gL}; the x-axis is along $C2$ while the y-axis corresponds to the axis of elongation of the FS and the z-axis deviates from C_3 by a small angle ψ which depends on the antimony concentration in the alloy.[2] The parameters Q_{11} characterize the $k\cdot p$ interaction of the valence band with the conduction band; α_c and α_v are inverse effective masses which take into account the influence of four more distant bands on the curvatures of the valence and conduction bands at the L-point. The contentration dependence of these parameters was determined in Ref. 2 and made more precise in Ref. 7 (Q_{ii} and α_i are given in atomic units):

$$\begin{aligned} &Q_{11}=0.457-0.188x,\ \alpha_v=1.1+0.7x,\\ &Q_{22}=0.03-0.04x,\ \alpha_c=0.615+0.4x,\\ &Q_{33}=0.344,\ E_{gL}=(10-242x)\ \text{meV}. \end{aligned} \quad (2)$$

The choice of the sign of the gap parameter E_{gL} is fundamental; for the parameter set (2), this sign is negative for $x > 0.04$. In this case, the dispersion law (1) implies that for $Q_{22}^2/\alpha_v < |E_{gL}|/2$ and $Q_{22}^2/\alpha_c < |E_{gL}|/2$, a saddle point must be present at the L point along k_y both in the conduction band and in the valence band. For the parameter set (2) this situation obtains for $x \gtrsim 0.15$. For smaller values of $|E_{gL}|$ the saddle point is absent, and the inverted character of the spectrum is manifested only by a flattening of the bottom of the conduction band (or the top of the valence band).

In analyzing the experimental data using the McClure model and the parameters (2) from Refs. 7 and 8, we were obliged to take into account the fact that the dependence on antimony concentration of the minimum cross section of the FS $S_{\min}^{(2)}(x)$ in the region $x \geqslant 0.15$ which we obtained differs somewhat both from the data in Ref. 2 and from the later, more precise data of Refs. 7 and 8 (Fig. 13). Therefore, in our calculations we used the choice of parameters (2) with corrected values of x chosen to fit our data;, e.g., we were able to match our data at $x = 0.27$ if we used the parameters

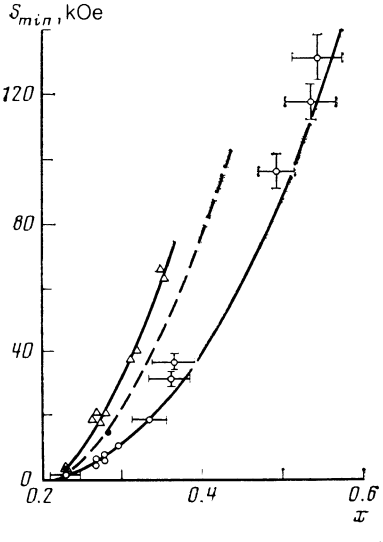

FIG. 13. Dependence of the non-central minimium cross sections in $Bi_{1-x}Sb_x$ alloys ($x \geqslant 0.22$) on antimony concentration: ○—data from Ref. 2, ●—from Refs. 7, 8, △—from the present work.

of (2) with $x = 0.29$. The function $E_{gL}(x)$ was taken to be the same as in Ref. 7 without any corrections, because it was derived from results given in several papers by various authors.

Equation (1) allows us to calculate the angular dependences of the extremal cross sections of isoenergetic surfaces at L for various Fermi energies (Figs. 2, 7), and also the variation with strain of the cross section $S_{\min}^{(1)}$ of the "neck" of the dumbbell, once we have found the variation $S_{\min}^{(2)}$ of the "body" of the dumbbell (Figs. 3, 9) from experiment. Calculations show that for a certain value $E_F = E_{cr}$ the angular dependence of the cross section, which previously was characteristic of a convex (ellipsoidal) isoenergetic surface (curve 1 in Fig. 2), splits into two sheets (the inset to Fig. 2); this implies a transition to the dumbbell–shaped FS. The calculated angular dependences of the FS cross sections are in good agreement with the experimental data, and describe both the variation of the FS with strain, including the transition to the dumbbell (Figs. 2, 3, and 9), and the fact that it is dumbbell-shaped under normal conditions in the alloy $Bi_{0.73}Sb_{0.27}$ (Fig. 7).

Especially worthy of attention is the good agreement between the theoretical and experimental dependences on the Fermi energy of the magnitude of the anisotropy in the group–I samples. The jump in the anisotropy in Fig. 4 occurs at the point E_{cr}, where two identical quasiellipsoids coalesce into one dumbbell-shaped isoenergetic surface, as a result of which the maximum cross section decreases by a factor of two. The process of coalescence is accompanied by the phenomenon of intraband magnetic breakdown (IB), which is observed for orientations of the magnetic field corresponding to the regions of maximum cross section.

4.3. Intraband magnetic breakdown

In contrast to interband magnetic breakdown (MB), the phenomenon of intraband magnetic breakdown (IB) is rare, and has been observed previously (besides in BI–Sb alloys[20,21]) only in the valence band of tellurium.[2] IB occurs when two or more isolated sheets of the FS belonging to a single band coalesce, in the process of which a conical point forms on the FS. The essential differences between MB and IB were discussed in Ref. 23, and consist of the following: (1) For IB, unlike for MB, there is always a variation in the direction of electron motion; (2) In IB, the breakdown probability satisfies $W \to 1/2$ as the magnetic field increases, whereas in MB we have $W \to +$ as $H \leftarrow \infty$; (3) It is significant that the characteristic fields for breakdown are different in the two cases: in the case of IB we have $H_B = \Delta E/\mu$, where ΔE is the magnitude of the potential barrier and $\mu = e\hbar/mc$ is the effective Bohr magneton, whereas MB occurs at considerably smaller magnetic fields:

$$H_B = (\Delta E)^2/E_F\mu \ll \Delta E/\mu.$$

In the process of formation of a dumbbell-shaped FS, there are two types of momentum-space paths which are located close enough to one another to admit the possibility of IB. One involves breakdown between the isolated quasiellipsoids for $E_F \lesssim E_{cr}$, while the other involves breakdown through the neck of the dumbbell as $H \to E_F \geqslant E_{cr}$, (see, e.g., the inset in Fig. 5). In the first case, the primary indication of IB should be doubling of the SdH oscillation frequencies from the maximum extremal cross sections of the FS quasiellipsoids in the region of high magnetic fields, while in the second case breakdown frequencies should appear against the background of high frequencies connected with the maximum cross sections of the dumbbell; these breakdown frequencies should be half as large as the background frequencies.

By invoking the dynamic variation of the FS with strain represented in the inset of Fig. 5, we can explain the strain dependence of the SdH oscillations originating from the maximum cross sections (see Fig. 6) as follows. The single frequency in curve 1 of Fig. 6 can be explained by the fact that the cross sections in the $k_x k_y$ plane of two isolated identical quasiellipsoids at the point L_1 are identically shaped. As the strain increases the Fermi level at L_1 rises, which leads to the approach of these two surfaces in wave vector space. When the spacing between the surfaces becomes sufficiently small, it becomes possible for an electron to tunnel through the potential barrier separating them when a magnetic field is present. The magnetic-breakdown trajectories formed in this way enclose approximately twice as large an area as the isolated trajectories, which leads to doubling of the frequency; this is apparent in curve 2 of Fig. 6 for fields $H > 30$ kOe, Curve 2 shows that the SdH frequency for low fields corresponds to isolated quasiclassical orbits, just as the oscillations in curve 1 of Fig. 6 do, while for high fields it corresponds to doubled magnetic-breakdown orbits. The doubled frequencies cannot be interpreted in terms of second harmonics or spin splittings, because in the large-strain region the experimental picture is reversed; in low magnetic fields the oscillations are determined by high-frequency components which come fron the maximum cross-section of the dumbbell, whereas a lower frequency appears in the large-H region (curve 5 in Fig. 6) because of breakdown through the neck of the dumbbell.

Under strain (which increases the neck of the dumbbell) the breakdown field H_B shifts to larger fields (see curves 4 and 5 in Fig. 6). An estimate of ΔE and μ based on the McClure model for a strain $\varepsilon = -2.5 \cdot 10^{-3}$ gives a value $H_B \approx 35$ kOe for the breakdown field through the neck of the dumbbell, which agrees with the form of the corresponding dependence of $\partial R/\partial H(H)$ in curve 5 of Fig. 6. In the strain region $(0.11 < \varepsilon < 0.17)\%$, for which the FS closely resembles a surface with a conical point, the quantization condition for the orbit in the direction of maximum cross section has the form[24,25]

$$S = 4\pi \frac{eH}{\hbar c}\left(n + \frac{1}{2} + \gamma_{1,2}\right), \tag{3}$$

where $S = S_1 + S_2$ is the total area, $S_1 = S_2$ is the area of each of the two individual regions after their coalescence ($E < E_{cr}$), and $\gamma_{1,2}$ is a correction to the quasiclassical energy levels. For $E_F \ll E_{cr}$, $\gamma_{1,2} = 0$, while for $E_F \gg E_{cr}$, $\gamma_{1,2} = \pm 1/4$, and for $E_F = E_{cr}$, $\gamma_{1,2} = \pm 1/8$. In the region of the conical point, i.e., $E_F \approx E_{cr}$, the Landau levels are pairwise equivalent, and in the general case the spacing between them in a magnetic field has an oscillatory correction.[25] This can cause high harmonics to appear in the interval of strains mentioned earlier (Fig. 5).

The strain ε_{cr} determines the onset of a change in the

connectivity of the FS; in Fig. 5 it is chosen to lie within a region where a conical point should exist. Although the value $\varepsilon_{cr} = 0.12\%$ is found at the lower boundary of this region, it is somewhat larger than the value of strain where, according to the McClure model, the neck of the dumbbell should form for this particular sample of $Bi_{0.78}Sb_{0.22}$ when $H = 0$ (Fig. 3). In terms of energy (estimated using the model of Ref. 17) this lack of agreement as to the value of the critical strain is equivalent to an indeterminacy in the position of the saddle point of $\Delta E \sim 3$ meV, and most likely can be connected with the variation of the spectrum and shift of the Fermi level in a magnetic field, i.e., the maximum cross sections in Fig. 5 were investigated at higher magnetic fields than the minimum cross sections in Fig. 3. Precise calculation of these effects is impossible because a model of the spectrum for $Bi_{1-x}Sb_x$ alloys with saddle points ($x > 0.15$) in a magnetic field does not exist. However, in this work, just as in the earlier work of Ref. 2, no frequency modulation effects were observed in the SdH oscillations for these alloys over a rather wide interval of magnetic fields. This indicates that the Fermi level shift in a magnetic field is small in this case.

From purely geometric considerations, IB between two isoenergetic surfaces can be observed in a range of angles bounded by those directions in which the planes perpendicualr to H are tangent to the conical portions of the surfaces; for the dumbbell-shaped surface, IB is observed up to the onset of disruption of the central cross section into two parts, corresponding to the body and neck of the dumbbell (see the inset to Fig. 5). In the case of a dumbbell-shaped FS which has just formed a neck ($E_F - E_{cr} \approx 2$ meV) the region of existence of IB is small and amounts to $\varphi \approx \pm 2°$ near the direction corresponding to maximum cross section of the dumbbell. As the neck of the dumbbell grows, the angular region in which IB exists widens, while the magnetic-breakdown frequencies become more than twice as small as the corresponding central cross-section frequencies. This is explained by the fact that as the cross section of the neck increases the breakdown field H_B grows, as a result of which a thin neck with small curvature breaks up into points increasingly far from $k_y = 0$. This effect is reflected in the bending down (in the direction of saturation) of the low-frequency branch in Fig. 5 for $\varepsilon > \varepsilon_{cr}$.

All the oscillatory dependence of the magnetoresistance was measured using longitudinal or transverse modulation of the magnetic field, and no special analysis of the oscillation amplitude under magnetic breakdown conditions was carried out. The absence of any noticeable falloff in amplitude as the magnetic field increases is apparently also characteristic of IB, and reflects the fact that for extremely large magnetic fields the "exit probability" for an electron onto the magnetic-breakdown orbit equals 1/2.

4.4. Anomalies in the thermoelectric power and resistivity

Recently there have been a number of theoretical and experimental papers predicting[10-13] and confirming[14-16] anomalous behavior of the thermoelectric power and resistivity in the neighborhood of an ETT. A singularity in the thermoelectric power α manifests itself in the form of a peak in the function $\alpha(z)$, where $z = E - E_{cr}$ parametrizes the nearness to the special point in the spectrum, i.e., the point where the connectivity of the FS changes. From the high-connectivity side of the FS, we have $\alpha(z) \propto |z|^{-1/2}$ (Refs. 11, 12); the resistivity has the appearance of a washed-out step.

The ETT observed in this work is related to the "bridge disruption" type of ETT. It is less studied than the other type of ETT, i.e., the "new sheet generation" type. The anomalies in the thermoelectric power which are observed in those group-I alloys ($x < x_{cr}$) which are close to the semiconductor–semimetal transition cannot be unequivocally related to the "bridge disruption" type of ETT.

For samples of the second type ($x \approx 0.27$, $E_F = 36$ meV) the overlap of the L and H terms is rather large, while the interval of achievable strain ($\sim 0.3\%$) is insufficient to cause the L terms to rise above the Fermi level. Therefore the negative-polarity peaks in the thermoelectric power which appear in Figs. 8b and 12 can only be related to passage of the Fermi level through a saddle point of the energy spectrum. In the case shown in Fig. 12, the position of the minimum as a function of $\alpha(\varepsilon)$ coincides with the critical strain for disruption of the dumbbell (Fig. 10), while in the case shown in Fig. 9b it agrees with the computed disappearance of the neck (Fig. 9a).

The sign of the anomaly in the thermoelectric power is of interest in its own right. In Ref. 13 it was shown that this sign is always opposite to the sign of the background thermoelectric power for carriers of the same sign which are far from the special point. From calculations for the system $Li_{1-x}Mg_x$ (Ref. 11) it also follows that the sign of the anomalies is positive for electrons and negative for holes for ETTs of both types. Although investigation of anomalies in the thermoelectric power for the "new sheet generation" type of ETT have confirmed this rule[15,16,27], a recently-observed negative-polarity anomaly for disruption of an electronic dumbbell does not agree with it. Apparently, in the general case the sign of the thermoelectric power anomaly is to a considerable degree determined by the scattering processes in a given system, as was pointed out in Ref. 28.

The anomaly in the resistivity observed in this work for disruption of the neck of a dumbbell (Fig. 12a) has the form of a washed-out step, which is in complete agreement with the theoretical calculations,[11,12]

5. CONCLUSION

In the $Bi_{1-x}Sb_x$ alloys under investigation here ($0.2 \leqslant x \leqslant 0.3$), the electronic FS which is close to the bottom of the L-extrema consists of two identical quasiellipsoids, which coalesce into a dumbbell for a certain critical value E_{cr}. This process, which constitutes an ETT of "bridge formation" type, is accompanied by anomalies in the thermoelectric power and resistivity, and in a magnetic field by intraband magnetic breakdown. The results obtained unequivocally attest to the presence of a saddle point in the spectrum of $Bi_{1-x}Sb_x$ alloys with $x \geqslant 0.2$ and to a negative direct gap E_{gL} in this region of antimony concentrations.

Our conclusion concerning the inverted character of the spectrum of $Bi_{1-x}Sb_x$ alloys for $x \geqslant 0.04$ allows us to explain a number of results which are not in agreement with previously-used models of the spectrum ($E_{gL} < 0$ in Bi). For example, the strong increase in the maximum cyclotron mass at the bottom of the band in $Bi_{1-x}Sb_x$ alloys for $x \approx 0.15$, as reported in Ref. 29, is not a consequence of a nonmomotonic dependence of the model parameters on

composition,[17] as stated in Ref. 29, but rather is connected with flattening of the bottom of the conduction band in the region in which the saddle point appears. The nonmonotonic behavior of the magnetoresistivity observed in Ref. 30 for **H** 11 C_2 in the alloys $Bi_{0.8}Sb_{0.2}$ and $Bi_{0.8}Sb_{0.2}Te_{0.001}$ can also be explained by assuming that the energy spectra of these compounds are inverted for this range of concentrations.

In conclusion, we take this opportunity to thank M. I. Kaganov, G. McClure, Ya. G. Ponomarev and I. I. Farbshtein for useful discussions.

[1)]The data of Ref. 4 which suggest that a saddle point is present in the spectrum of pure bismuth under hydrostatic compression must be considered erroneous.

[2)]The results of Ref. 16, in which the "bridge disruption" ETT identified in oscillations of the thermoelectric power was accompanied by a singularity in the resistivity, have been unique up until now.

[3)]In alloys of any given composition this deviation does not exceed 3.5° (Ref. 4).

[4)]In Ref. 2, oscillations from the hole FS in the alloy $Bi_{0.75}Sb_{0.25}$ appeared for $H \gtrsim 80$ kOe. Apparently, the high field explains why they were not observed in this work.

[1]F. M. Muntyanu and M. I. Onu, *Material from the 3rd on Current Problems in the Physics of Semimetals and Narrow-Gap Semiconductors* Kishinev: ShTIINTsA, 1987, p. 15.
[2]N. B. Brandt, R. Germann, G. I. Golysheva *et al.*, Zh. Eksp. Teor. Fiz, **83**, 2152 (1982) [Sov. Phys. JETP **56**, 1247 (1982)].
[3]N. B. Brandt, S. M. Chudinov, and V. G. Karavaev, Zh. Eksp. Teor. Fiz. **70**, 2296 (1976) [Sov. Phys. JETP **43**, 1198 (1976)].
[4]N. B. Brandt, V. V. Moshchalkov, and S. M. Chudinov, Zh. Eksp. Teor. Fiz. **14**, 1829 (1978) [Sov. Phys. JETP **47**, 953 (1978)].
[5]L. A. Farbshtein, Usp. Fiz. Nauk **149**, 336 (1986) [Sov. Phys. Usp. **29**, 577 (1986)].
[6]V. S. Edel'mann, Uap. Fiz. Nauk **123**, 257 (1977) [Sov. Phys. Usp. **20**, 819 (1986)].
[7]Ya. G. Ponomarev and M. V. Sudakova, Material from the 7th All-Union Symposium on Narrow-Gap Semiconductors and Semimetals. Part 2, L'vov, 1986, p. 164.
[8]M. V. Sudakova, Nguyen Minh Thu, K. N. Kashirin, and Ya. G. Ponomarev, Material from the 3rd School on Current Problems in the Physics of Semimetals and Narrow-Gap Semiconductors, Kishinev: ShTIINTsA, 1987, p. 18.
[9]N. B. Brandt, R. Germann, V. A. Kul'bachinskii *et al.*, Fiz. Tverd. Tela (Leningrad) **24**, 1966 (1982) [Sov. Phys. Solid State **24**, 1122 (1982)].
[10]I. M. Lifshits, Zh. Eksp. Teor. Fiz. **38**, 1569 (1960) [Sov. Phys. JETP **11**, 1130 (1960)].
[11]V. G. Vaks, A. V. Trefilov, and S. B. Fomichev, Zh. Eksp. Teor. Fiz. **80**, 1613 (1981) [Sov. Phys. JETP **53**, 830 (1981)].
[12]A. A. Varlamov and A. V. Pantsulaya, Zh. Eksp. Teor. Fiz. **89**, 2188 (1985) [Sov. Phys. JETP **62**, 1263 (1985)].
[13]A. A. Abrikosov, A. A. Varlamov, and A. V. Pantsulaya, Preprint No. 656, Institute of Theoretical Physics, Univ. of Wroclaw, 1986, p. 37.
[14]Yu. P. Gaidukov, N. P. Danilova, and E. V. Nikiforenko, Pis'ma Zh. Eksp. Teor. Fiz. **39**, 522 (1984) [JETP Lett. **39**, 637 (1984)].
[15]N. B. Brandt, V. S. Egorov, M. Yu. Lavrenyuk, N. Ya. Minina, and A. M. Savin, Zh. Eksp. Teor. Fiz. **89**, 2257 (19085) [Sov. Phys. JETP **62**, 1303 (1985)].
[16]D. R. Overcash, T. Davis, J. W. Cook and M. J. Skove, Phys. Rev. Lett. **46**, 287 (1981).
[17]J. W. McClure and K. H. Choi, Solid State Commun. **21**, 1015 (1977); J. W. McClure, J. Low Temp. Phys. **25**, 257 (1976).
[18]H. Berger, B. Christ, and J. Troshke, Crystal Res. and Technol. **17**, 1233 (1982).
[19]D. V. Gitsu, F. M. Muntanyu, and M. I. Onu. Phys. Status Solidi **B105**, K95 (1981).
[20]N. B. Brandt, G. I. Golysheva, Nguyen Minh Thu *et al.*, Fiz. Nizk. Temp. **13**, 1209 (1987) [Sov. J. Low Temp. Phys. **13**, 683 (1987)].
[21]M. Yu. Lavrenyuk, N. Ya. Minina, and A. M. Savin, Pis'ma Zh. Eksp. Teor. Fiz. **46**, 224 (1987) [JETP Lett. **46**, 282 (1987)].
[22];V. B. Anzin, M. S. Bresler, I. I. Farbstein *et al.*, Phys. Stat. Sol. **40**, 417 (1970).
[23]I. M. Lifshits, M. Ya. Azbel', and M. I. Kaganov, *Elekt 5onnaya Teoriya Metallov* (*Electron Theory of Metals*, Consultants Bureau, New York, 1973), Moscow: Nauka, 1971.
[24]G. E. Zil'berman, Zh. Eksp. Teor. Fiz. **34**, 748 (1958) [Sov. Phys. JETP **7**, 512 (1958)].
[25]M. Ya. Azbel', Zh. Eksp. Teor. Fiz. **39**, 1276 (1960) [Sov. Phys. JETP **12**, 891 (1960)].
[26]V. S. Egorov and A. N. Fedorov, Zh. Eksp. Teor. Fiz. **85**, 1647 (1983) [Sov. Phys. JETP **58**, 959 (1983)].
[27]N. V. Zavaritskii, V. M. Makarov, and A. A. Yurgens, Pis'ma Zh. Eksp. Teor. Fiz. **42**, 148 (1985) [JETP Lett. **42**, 182 (1985)].
[28]M. G. Bondarenko, M. S. Vas'kin, V. M. Grabov *et al.*, Material from the 3rd School on Current Problems in the Physics of Semimetals and Narrow-Gap Semiconductors, Kishinev: ShTIINTsA, 1987, p. 6.
[29]B. Fellmuth, H. Kruger, R. Rudolf, and K. Hermann, Phys. Stat. Solidi **B106**, 561 (1981).
[30]D. V. Gitsu, M. Glinski, and F. M. Muntyanu, Fiz. Tverd, Tela (Leningrad) **19**, 1450 (1977) [Sov. Phys. Solid State **19**, 843 (1977)].

Translated by Frank J. Crowne